Second-Harmonic Light Generation in Crystals with Natural Optical Activity*

H. J. SIMON AND N. BLOEMBERGEN
Gordon McKay Laboratory, Harvard University, Cambridge, Massachusetts
(Received 12 February 1968)

Whenever a circularly polarized laser beam propagates along an axis of threefold symmetry in a piezoelectric crystal, the second-harmonic polarization is circularly polarized in the opposite sense. Rabin and Bey have discussed the theory of second-harmonic generation in crystals with natural optical activity. We have observed this circular polarization and also the difference in coherence lengths for opposite senses of circular polarization, with both fundamental and second-harmonic beams propagating along the [111] direction in single crystals of $NaClO_3$ and $NaBrO_3$, belonging to the cubic class 23, for which the proper eigenmodes are circularly polarized waves. The nonlinear susceptibility of both $NaClO_3$ and $NaBrO_3$ has been measured and compared with the nonlinear susceptibility of α-quartz. The relative sign of the susceptibilities has been determined in second-harmonic interference experiments with the same laser beam traversing two crystals in succession. The interesting questions of the sign of the nonlinear susceptibility, piezoelectric constant, optical activity, and the absolute atomic configuration of the antipodes are discussed. The question of conservation of angular momentum is resolved by taking into account the crystalline-field potential of threefold symmetry, which gives rise to a torque on the crystal lattice.

1. SYMMETRY CONSIDERATIONS FOR HARMONIC GENERATION BY CIRCULARLY POLARIZED LIGHT

THE symmetry properties of second-harmonic generation are described by a symmetric third-rank nonlinear susceptibility tensor which has the same properties as the piezoelectric tensor. When sum or difference frequencies are generated, the nonlinear susceptibility tensor may have antisymmetric parts in all pairs of indices. Complete tabulations have been given by Giordmaine[1] and Butcher.[2] The third-harmonic generation is described by a fourth-rank tensor, which is symmetric for permutation of three indices. Complete expressions have been given by Maker *et al.*[3] When other combination frequencies are considered in this order of nonlinearity, the tensors may have antisymmetric parts in those pairs of indices which correspond to distinguishable field components. When optical dispersion may be ignored, the tensors must be symmetric for all permutations of the indices, as stated by Kleinman.[4]

With these general tensors, the components of the harmonic polarization may be calculated for any state of polarization of the incident laser beam. For elliptic and circular polarization some of the fundamental field components must be written as complex quantities. The resulting nonlinear polarization will in general create an elliptically polarized harmonic wave.

Consider, however, the case that the incident light wave (or waves) is (are) circularly polarized and propagating along a three-, four-, or sixfold axis of symmetry. The resulting harmonic (or combination frequency) wave must either vanish or also be circularly polarized around this direction, because the rotational symmetry of the combined system, crystal and electromagnetic field, must be preserved. As will be shown explicitly in Sec. 4 of this paper, the change in angular momentum of the electromagnetic field around an axis of m-fold symmetry is either 0 or $\pm m\hbar$.

This implies that the second-harmonic wave generated by a circularly polarized laser beam propagating along a threefold axis is circularly polarized in the opposite sense. This may be verified by explicit calculation from the nonlinear susceptibility tensors for the [111] direction in the cubic classes $\bar{4}3m$ and 23, and for the axis of symmetry in the trigonal piezoelectric classes and the hexagonal classes.

When the circularly polarized light propagates along a fourfold axis, the second harmonic vanishes. The third harmonic will be circularly polarized in the opposite sense in this case. This may again be verified by explicit calculation for light propagating along [100] directions in cubic crystals with a fourfold axis, and in tetragonal classes. The third harmonic must vanish when the fundamental light is circularly polarized around a three- or sixfold axis, or in fluids.

The extension of these considerations to other combination frequencies is straightforward. If, for example, an incident light wave ω_1 is left circularly polarized and an incident light wave at $\omega_2 > \omega_1$ is right circularly polarized around a trigonal axis, only a left circularly polarized wave at the difference frequency $\omega_2 - \omega_1$ can be generated.

The geometries in which only circularly polarized light waves occur are of particular importance in the case of crystals with natural optical activity. In the cubic crystals of the class 23, the proper zero-order polarization modes for light propagating in any direction are the two circularly polarized modes, which

* Supported by the Signal Corps of the U. S. Army, the Office of Naval Research, and the U. S. Air Force.
[1] J. A. Giordmaine, Phys. Rev. **138**, A1599 (1965).
[2] P. N. Butcher, Bulletin 200, Engineering Experiment Station, Ohio State University, Columbus, 1965 (unpublished).
[3] P. D. Maker, R W. Terhune, and C. M. Savage, in *Proceedings of the Third International Conference on Quantum Electronics*, edited by P. Grivet and N. Bloembergen (Dunod Cie., Paris, 1964), p. 1559.
[4] D. A. Kleinman, Phys. Rev. **126**, 1977 (1962).

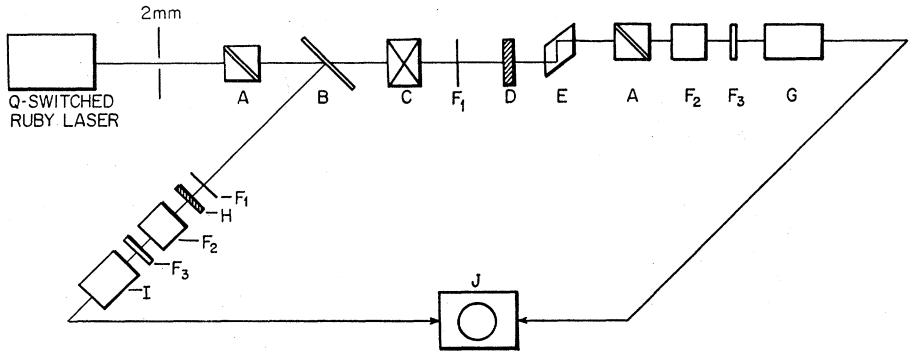

FIG. 1. Experimental arrangement for creating circularly polarized laser light and analyzing and detecting circularly polarized second-harmonic light. [A, Glan-Kappa polarizer; B, beam splitter (35% reflectance mirror); C, quartz $\frac{1}{4}\lambda$ plate; D, optically active crystal; E, Fresnel rhomb; F_1, Corning filter CS 2–64; F_2, $CuSO_4$ cell; F_3, 347 mμ interference filter; G, EMI 9634 photomultiplier; H, reference quartz platelet; I, EMI 6255B photomultiplier; J, Tektronix type 555 dual-beam oscilloscope.]

propagate with different velocities. This difference is of course proportional to the specific optical activity. When the nonlinear susceptibility for second-harmonic generation in crystals of this class is to be determined, two different coherence lengths will occur, in general, in the formula for the second-harmonic intensity through a plane parallel slab,

$$L_{\mathrm{coh}}^{\pm}=\frac{\pi c}{2\omega}\frac{1}{[n^{\pm}(2\omega)-n^{\mp}(\omega)]}. \quad (1)$$

For arbitrary geometries the incident wave must be decomposed into circularly polarized modes, and the resulting second-harmonic waves must be recombined to a wave whose polarization and intensity is a rather inconvenient function of the thickness of the slab. Experimental data which can be quantitatively interpreted should, therefore, be taken preferably with a circularly polarized laser beam propagating along the [111] direction. In that case, the emerging second-harmonic beam is always circularly polarized in the opposite direction and the intensity variation is described by a single coherence length.

In Sec. 2 of this paper the experimental arrangement is described which allows the determination of the magnitude of the nonlinear susceptibilities of $NaClO_3$ and $NaBrO_3$ crystals which both have 23 symmetry. The relative sign can be determined from interference experiments which are described in Sec. 3.

If the light is propagating along the trigonal axis in α-quartz, the same considerations apply. In fact, the theoretical discussion of Rabin and Bey[5] applies explicitly to this geometry. We have verified their predictions experimentally. For propagation in directions which make an angle with the optic axis, the proper eigenmodes are, or course, essentially linearly polarized, although strictly speaking they would have some ellipticity. The latter effect is small and experimentally unobservable so that the previous determinations of the optical nonlinearity in α-quartz with linearly polarized light are, of course, correct.

In the elementary scattering process, in which two right circularly polarized quanta at the fundamental frequency are transformed into one left circularly polarized quantum at the second-harmonic frequency, the angular momentum of the electromagnetic fields changes by three units, $3\hbar$. Since the crystal is nonabsorbing and its electronic wave functions are unchanged, this raises the question of conservation of angular momentum. In the last section of this paper a discussion of this question is presented, which supplements some previous remarks.[6]

2. SECOND-HARMONIC GENERATION EXPERIMENT IN $NaClO_3$ AND $NaBrO_3$

A. Preparation of Samples

All dextrorotatory crystals of $NaClO_3$ and $NaBrO_3$ were grown from water solution by standard rocking techniques.[7] Optical polishing was done on a nonwoven polishing cloth with kerosene lubricant and 0.3-μ aluminum oxide abrasive. A hard wax lap could not be used because of the difficulty in finding a suitable lubricant that would not simultaneously dissolve either the wax or the crystal. Flatness of individual faces was typically 0.5–1 μ over an area of a quarter-inch square. Parallelism of the two platelet faces was typically 2–6 μ over the same area as measured with an air gauge. The most useful measurement of the quality of the polishing was the experimental ratio of peak second harmonic to minimum second harmonic. At best this ratio was from 10:1 to 20:1, although quite often it was less. A levorotatory sample was cut from the same crystal used by Collins.[8]

[5] H. Rabin and P. P. Bey, Phys. Rev. **156**, 1010 (1967).

[6] N. Bloembergen, Technical Report No. 544, Harvard University, 1967 (unpublished); J. Phys. (Paris) (to be published).

[7] A. N. Holden and P. Singer, *Crystals and Crystal Growing* (Doubleday, New York, 1960).

[8] F. A. Collins and N. Bloembergen, J. Chem. Phys. **40**, 3479 (1964).

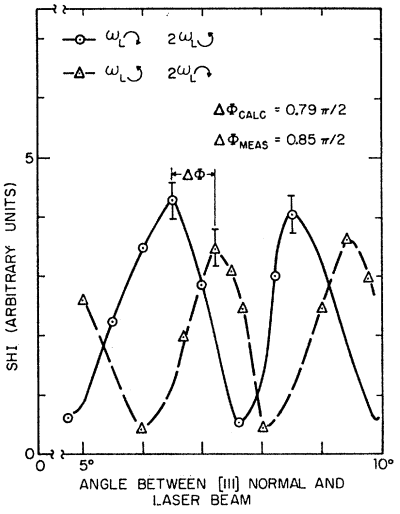

FIG. 2. Circularly polarized second-harmonic light intensity (SHI) in a 5.2-mm-thick $NaClO_3$ platelet versus angle between the [111] normal and the laser axis, for right and left circularly polarized laser light.

B. Experimental Arrangement

The beam of a pulsed ruby laser was given a circular polarization by means of a Glan-Kappa polarizer and a $\frac{1}{4}\lambda$ compensated quartz plate. The polarization of both the fundamental and harmonic beam emerging from the sample could be checked by means of a Fresnel rhomb and Glan-Kappa prism as analyzer. The experimental arrangement, which is fairly standard in all other respects, is shown in Fig. 1. Each pulse of the Q-switched ruby laser was monitored by means of a 35% reflectance dielectric-coated mirror as a beam splitter and a quartz sample as a reference for second-harmonic generation. A typical pulse had an energy content of 0.1 J and a duration of 3×10^{-8} sec. The diameter of the beam passing through the samples was 2 mm. $CuSO_4$ solutions and interference filters to eliminate the fundamental light preceded photomultipliers. The traces of the second-harmonic pulses were displayed simultaneously on a Tektronix 555 dual-beam oscilloscope.

When the light beams were within 1° of the [111] crystallographic direction, it was verified that the second-harmonic polarization was circularly polarized in the opposite sense from the fundamental. The observed ratio of the major and minor polarization axis was 1:0.97.

C. Coherence Lengths

The transmitted second-harmonic light (SHI) generated in a plane parallel platelet goes as

$$I(2\omega)\sim\sin^2[(L/L_{\rm coh}{}^{\pm})\tfrac{1}{2}\pi],$$

where L is the optical path length in the crystal. For the two opposite circular polarizations of the laser beam the difference in phase angle of this factor is

$$\Delta\Phi=\left(\frac{L}{L_{\rm coh}{}^{+}}-\frac{L}{L_{\rm coh}{}^{-}}\right)\frac{\pi}{2}=\frac{\Delta L_{\rm coh}}{L_{\rm coh}}\frac{L}{L_{\rm coh}}\frac{\pi}{2}. \quad (2)$$

Now

$$\frac{\Delta L_{\rm coh}}{L_{\rm coh}}\approx\frac{\delta n}{\Delta n}=\frac{\text{(rotary birefringence)}}{\text{(optical dispersion)}}\approx\frac{1}{10^3}$$

in $NaClO_3$. For a platelet approximately a thousand coherence-lengths thick, the difference in the phase angle for the two polarization cases is approximately $\frac{1}{2}\pi$. This result is shown in Fig. 2, where a $NaClO_3$ platelet, 5 mm thick, was turned from the laser axis for the two cases of laser circular polarization.

Similar results were obtained for a $NaBrO_3$ crystal as shown in Fig. 3. If linearly polarized light is used, the observed second-harmonic intensity varies as the sum of the curves for the two circular polarizations. This is verified by the experimental data in Fig. 4. Clearly such curves are less suitable for a quantitative determination of the nonlinear susceptibility.

An α-quartz crystal was cut into a platelet with the optic axis in the normal direction. The circularly polarized nature of the second harmonic was again verified in this case and its magnitude allowed a simple comparison of the nonlinearities of $NaClO_3$ and $NaBrO_3$ with the known nonlinear constant in quartz.

D. Magnitude of Nonlinear Susceptibility

If the real amplitude of a circularly polarized wave propagating along the [111] direction is A_0, the components of the field with respect to the cubic axes are

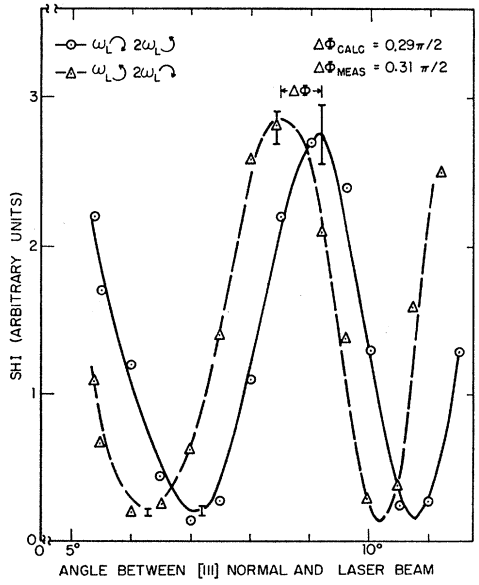

FIG. 3. Circularly polarized SHI in a 1.8-mm-thick $NaBrO_3$ platelet versus angle between the [111] normal and the laser axis for right and left circularly polarized laser light.

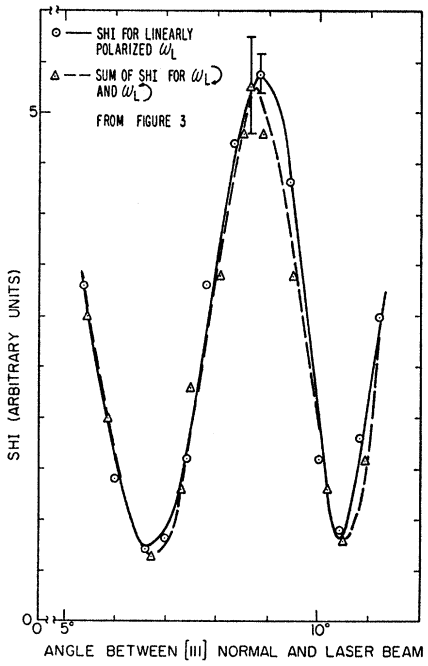

FIG. 4. SHI in a 1.8-mm-thick $NaBrO_3$ platelet versus the angle between the [111] normal and the laser axis, for linearly polarized laser light. The sum of right and left circularly polarized laser light from Fig. 3 is also plotted as the solid line.

expressed as follows:

$$E_x = 2^{-1/2}A_0\cos\omega t - 6^{-1/2}A_0\sin\omega t,$$
$$E_y = -2^{-1/2}A_0\cos\omega t - 6^{-1/2}A_0\sin\omega t, \quad (3)$$
$$E_z = (2/3)^{1/2}A_0\sin\omega t.$$

The resulting second-harmonic polarization has the coordinates

$$P_x = \chi_{14}E_xE_y = \chi_{14}A_0^2[-\tfrac{1}{2}3^{-1/2}\sin 2\omega t - \tfrac{1}{6}\cos 2\omega t],$$
$$P_y = \chi_{25}E_zE_x = \chi_{14}A_0^2[+\tfrac{1}{2}3^{-1/2}\sin 2\omega t - \tfrac{1}{6}\cos 2\omega t], \quad (4)$$
$$P_z = \chi_{36}E_xE_y = -\tfrac{1}{3}\chi_{14}A_0^2\cos 2\omega t.$$

This corresponds to a circular harmonic polarization precessing in the opposite direction with a real amplitude $6^{-1/2}\chi_{14}A_0^2$.

It is advantageous to express the field in terms of a complex amplitude $Ae^{-i\phi}$, where $A=\frac{1}{2}A_0$. Furthermore, the more explicit third-rank tensor elements $\chi_{xyz}=\chi_{xzy}=\chi_{zxy}=\chi_{zyx}=\chi_{yxz}=\chi_{yzx}$ are introduced, such that $\chi_{14}=\chi_{xyz}+\chi_{xzy}$. This notation is the same as that adopted by Robinson.[9]

In terms of a coordinate system $\hat{u}$, $\hat{v}$, $\hat{w}$ with $\hat{u}$ parallel to [111] direction, $\hat{v}$ parallel to $[\bar{1}\bar{1}2]$, and $\hat{w}$ parallel to $[1\bar{1}0]$ the fundamental field may be written as

$$\mathbf{E}(\omega) = A(\hat{v}+i\hat{w})e^{-i\omega t-i\phi} + \text{c.c.}, \quad (3')$$

and the harmonic polarization is

$$\mathbf{P}(2\omega) = 2^{3/2}3^{-1/2}\chi_{xyz}A^2(\hat{v}-i\hat{w})e^{-2i\phi}e^{-2i\omega t} + \text{c.c.} \quad (4')$$

The phase factor ϕ indicates the instantaneous direction of $\mathbf{E}(\omega)$ and $\mathbf{P}(2\omega)$. For $\phi=0$ both vectors are parallel to $\hat{v}$ and lie in the $(1\bar{1}0)$ symmetry plane. They also are parallel in the equivalent planes $(10\bar{1})$ and $(0\bar{1}1)$ obtained by a rotation of $\pm 120°$ around the [111] axis.

The amplitude of the circularly polarized harmonic polarization in α-quartz, induced by a fundamental field circularly polarized around the trigonal axis,

$$\mathbf{E}(\omega) = A(\hat{x}+i\hat{y})e^{-i\phi}e^{-i\omega t} + \text{c.c.},$$

is given by

$$\mathbf{P}(2\omega) = 2\chi_{xxx}A^2(\hat{x}-i\hat{y})e^{-2i\phi}e^{-2i\omega t} + \text{c.c.}$$

The vectors rotate in opposite directions and pass each other along the $\hat{x}$ axis and the equivalent directions obtained by turning the $\hat{x}$ axis by $\pm 120°$.

Comparison of the maxima in the harmonic-generation curves, in combination with the known coherence lengths, leads to the values of χ_{xyz} in $NaClO_3$ and $NaBrO_3$ relative to the known value of χ_{xxx} in quartz. The pertinent data are compiled in Table I. The values of Miller's ratio Δ, as defined by Robinson, are also listed. This factor Δ is obtained by multiplying the nonlinear susceptibility by $(4\pi)^3[n^2(\omega)-1]^{-2}[n^2(2\omega)-1]^{-1}$. The large variation in the factor Δ for the two isomorphous cubic crystals $NaClO_3$ and $NaBrO_3$ with nearly identical atomic structures is striking. It shows that Miller's empirical rule that Δ is approximately constant can be violated rather drastically.[10] This will become even more apparent in the next section, where the relative signs of χ_{14} for $NaClO_3$ and $NaBrO_3$ are shown to be opposite for the same sense of the atomic configuration.

Early observations by Savage and Miller[11] in $NaClO_3$ and $NaBrO_3$ are in qualitative agreement with the quantitative determination of the nonlinear suscepti-

TABLE I. Summary of linear and nonlinear optical data at the frequency of the ruby laser and its second harmonic.

Crystal	Second-harmonic coefficient (10^{-9} esu)	Miller's ratio Δ (10^{-6} esu)	Index of refraction[a] $n(\omega)$	$n(2\omega)$	Optical activity[a] deg/mm at ω	at 2ω
α-quartz	$\chi_{xxx}=2.5$[b]	1.9[b]	1.541	1.566	15	70
$NaClO_3$	$\chi_{xyz}=3.3$	3.0	1.512	1.540	2.2	9.3
$NaBrO_3$	$\chi_{xyz}=1.35$	0.63	1.611	1.661	1.4	11.6

[a] The linear optical data are taken from Landolt-Bornstein, *Zahlenwerte und Funktionen, Bd.2, Tl.8*, (Julius Springer-Verlag, Berlin, 1936). Where necessary, interpolated values were obtained by means of the Cauchy dispersion function, as discussed, e.g., on p. 468 of Ref. 15.
[b] From Ref. 9.

[9] F. N. H. Robinson, Bell System Tech. J. **47**, 913 (1967).

[10] The significance of Miller's rule is solely that it describes the gross trend of χ^{NL} with increasing linear susceptibility. The broad statistical distribution of Δ values found in Ref. 9 confirms that variations in Δ of one order of magnitude may be expected in general. The theoretical models discussed in this reference would, however, not predict such a large variation for the isomorphous crystals $NaClO_3$ and $NaBrO_3$.

[11] A. Savage and R. C. Miller, Appl. Cpt. **1**, 661 (1962).

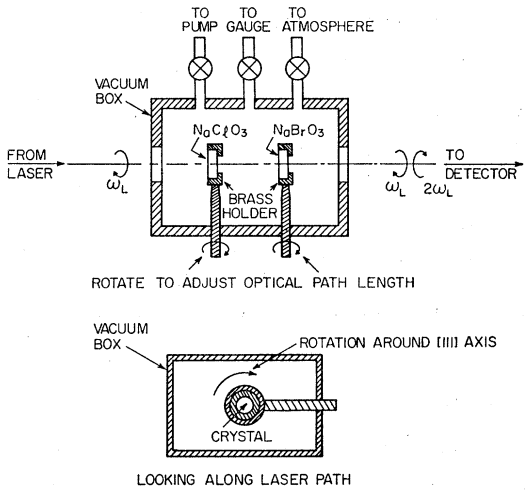

FIG. 5. Experimental arrangement for creating interference of circularly polarized SHI in $NaClO_3$ and $NaBrO_3$. The air pressure in the path between the crystals can be varied.

bilities reported here. It should be pointed out that the absolute value of the nonlinearity could also have been obtained simply by using a wedge-shaped sample.[12] In this case no particular attention has to be paid to the nature of the polarization or the existence of two coherence lengths. The observed output corresponds to the average of the curves displayed in Figs. 2 and 3. Wedge-shaped samples would, however, not permit the interference experiments described in the following section, nor the determination of the relative sign of the nonlinearity.

3. INTERFERENCE EXPERIMENTS

When second-harmonic radiation is generated by the same laser beam in two consecutive samples, a definite phase relationship exists between the two sources of harmonic radiation. Such interference experiments have been carried out successfully[13] to determine the phase of the complex nonlinear susceptibility in absorbing media. Even in nonabsorbing media, where χ^{NL} is real, an ambiguity in the sign still exists. It is physically clear that two piezoelectric antipodes, i.e., two crystals which are inversion images of each other, will have opposite signs in all elements of the third-rank tensor property. In the same manner a $NaClO_3$ with left-handed optical activity will have an opposite sign of the susceptibility from the right-handed optical antipode. It is *a priori* not determined whether left-handed $NaBrO_3$ or left-handed α-quartz will have the same sign as left-handed $NaClO_3$, or the opposite.

The experimental arrangement for the interference effects between two samples is shown in Fig. 5. The two crystal platelets are mounted in a vacuum box. Each crystal can be individually turned around an axis perpendicular to the laser beam to vary its optical path length. Suppose that the first crystal is dextrorotatory $NaClO_3$ so adjusted as to give a maximum harmonic generation according to a curve in Fig. 2. Now another dextrorotatory $NaClO_3$ platelet is placed in the laser beam in the evacuated box, in exactly the same crystallographic orientation. This is of course entirely equivalent, except for Fresnel reflections, to making the first crystal thicker. As a result, the second-harmonic intensity with both crystals in the box must be lower. In fact, when the second crystal is individually adjusted to give by itself alone a maximum second-harmonic intensity,

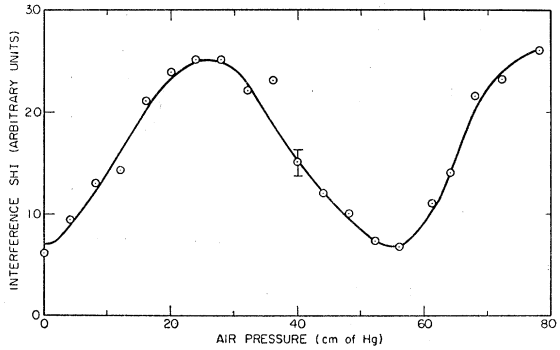

FIG. 6. Second-harmonic interference intensity from two dextrorotatory $NaClO_3$ (111) crystals versus the air pressure.

the two crystals together will give almost zero intensity. A slight harmonic signal may still be expected, because the intensity of the laser beam in the second crystal will be slightly lower due to Fresnel reflection and other possible optical losses. When the air is admitted into the vacuum box, the dispersion of the air between the two crystals will cause a phase variation between the harmonic fields and the second-harmonic amplitude from the two platelets may be twice as high, or the intensity four times as high, as that of a single platelet. This interference effect is shown in Fig. 6. Sharp zeros and four times individual crystal peak intensities are not observed because of poor ratios of peak second-harmonic intensity to minimum second-harmonic intensity in the individual crystals.

There is another way to create a phase difference between the two $NaClO_3$ crystals. In this method the two crystal plates are kept in vacuum and parallel to each other, but the second $NaClO_3$ crystal is rotated around its own normal, i.e., the [111] direction in which the laser beam propagates. As remarked in the preceding section, the rotating harmonic polarization and the rotating laser field vector must cross the $(1\bar{1}0)$ plane at the same time. As this plane is turned, a phase shift between the harmonic source and fundamental field is induced. The threefold nature of the axis, as well as the oppositely rotating vectors at circular frequencies ω and 2ω, respectively, show immediately that the result-

[12] A. Savage, J. Appl. Phys. **36**, 1496 (1965).
[13] R. K. Chang, J. Ducuing, and N. Bloembergen, Phys. Rev. Letters **15**, 6 (1965).

ing interference pattern as a function of the angle of rotation around [111] has a period of 120°, in agreement with the experimental result shown in Fig. 7.

Still another possibility to cause a relative phase shift of π in the harmonic field of the second crystal is to turn this crystal 180° around an axis normal to the [111] direction. This flip-over of the second crystal changes second-harmonic interference maxima to minima and vice versa. If the turning is done around the $[1\bar{1}0]$ direction, the mathematical transformation is described by $x \rightarrow -y$, $y \rightarrow -x$, and $z \rightarrow -z$. Although this turning does not change the "handedness" of the crystal, it clearly changes the sign of the piezoelectric voltage with respect to a laboratory frame. If a compression along the [111] direction first caused the "front" face of the crystal to be positive, after the turning the back face will be positive. In the same manner second-harmonic polarization is flipped with respect to the laboratory frame.

A. Sign of Odd-Rank Tensors and Absolute Atomic Configuration of Optical Antipodes

In principle, the two dextrorotatory crystals may be aligned with their cubic axes parallel to each other by

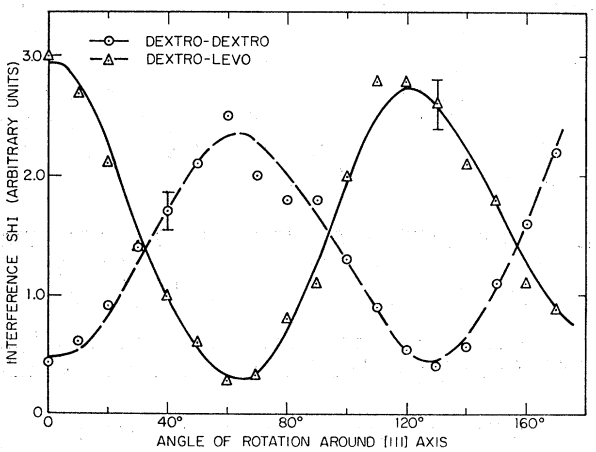

FIG. 7. Second-harmonic interference intensity from a pair of two dextrorotatory $NaClO_3$ (111) crystals and a pair of one dextrorotatory and one levorotatory $NaClO_3$ (111) crystals versus relative rotation around the [111] axis.

standard x-ray techniques. The distinction between the "front" (111) and "back" $(\bar{1}\bar{1}\bar{1})$ orientation should show as a minor asymmetry in the intensity of x-ray diffraction spots. In practice, it is preferable to determine the orientation of the (111) platelets by a Laue back scatter technique and by paying attention only to the gross symmetry of the pattern.

The question of the "front" or "back" orientation is decided separately by measuring the sign of the piezoelectric voltage, when the platelets are compressed.

All sign questions have to be reversed once more, if the second crystal has the opposite sense of optical activity. It was indeed verified that two platelets of $NaClO_3$, which are crystallographic antipodes, have indeed the opposite sign of χ_{xyz} as shown in Fig. 8. The piezoelectric constants have, of course, the opposite sign also, and when the cubic axes of the two crystals are parallel in space, the piezoelectric voltages under compression are opposite.

Bijvoet and collaborators[14] have been able to determine the absolute atomic configuration belonging to each antipode by the technique of anomalous x-ray scattering. If the x-ray scattering factor of an atom becomes complex, the hkl and $\bar{h}\bar{k}\bar{l}$ diffraction spots may have a different intensity.

They discovered that a $NaBrO_3$ crystal with the same absolute atomic configuration A, shown in Fig. 8, as a $NaClO_3$ crystal has the opposite sense of natural optical activity. This is in agreement with an ancient observation that right-rotating $NaBrO_3$ grows epitaxially on left-rotating $NaClO_3$. We have verified that such crystals have the same sign of the piezoelectric voltage. In other words, the same absolute configurations of $NaBrO_3$ and $NaClO_3$ have the same sign of the piezoelectric constant, in agreement with a simple mechanical ionic model for the piezoelectric effect described by Mason.

All of the above orientation factors are schematically displayed in Fig. 9. Optical rotary direction is measured with the standard convention[15]; i.e., a dextrorotatory crystal rotates the polarization clockwise when viewed looking toward the light source. For dextrorotatory $NaClO_3$ Collins[8] and Mason[16] have shown that the positive (111) face develops a positive voltage under the influence of a tensile stress, which is counted as positive. A piezoelectric voltage measurement plus a back reflection x-ray Laue photograph allowed an unambiguous orientation of the $NaClO_3$ crystal. Since Bijvoet[14]

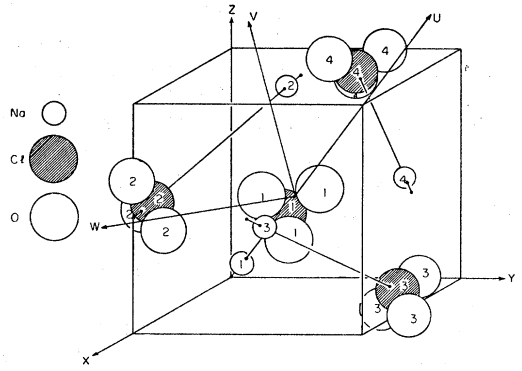

FIG. 8. Crystal structure A of dextrorotatory $NaClO_3$ and levorotatory $NaBrO_3$, taken from Refs. 8 and 14.

[14] G. Beurskens-Kerssen, J. Kroon, H. J. Endeman, J. van Laar, and J. M. Bijvoet, *Crystallography and Crystal Perfection* (Academic Press, London, 1965), p. 225; G. Beurskens-Kerssen, Academisch Proefschrift, Utrecht, 1963 (unpublished).

[15] F. A. Jenkins and R. H. White, *Fundamentals of Optics* (McGraw-Hill Book Co., New York, 1957).

[16] W. P. Mason, Phys. Rev. **70**, 529 (1946).

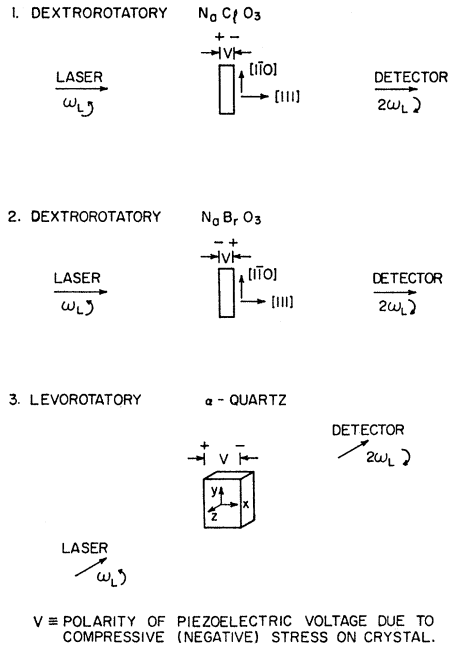

FIG. 9. Schematic diagram of unambiguous orientation of $NaClO_3$, $NaBrO_3$, and α-quartz crystals.

has shown that dextrorotatory $NaBrO_3$ has the inverted atomic structure of dextrorotatory $NaClO_3$, we assigned the positive (111) face to that face which developed a negative voltage under the influence of a positive tensile stress. For the levorotatory α-quartz we followed the IEEE convention[17]: "On extension, the positive ends of the a axes, and therefore of the X axes, become negatively charged with right quartz, positively charged with left quartz." Absolute orientation of this crystal from piezoelectric voltage measurements agreed with absolute orientation from the natural faces. The absolute atomic configuration of α-quartz was determined by de Vries.[18]

The question of the sign of the nonlinear susceptibility for these crystals becomes, therefore, intriguing. The result of a second-harmonic interference experiment with a $NaClO_3$ and a $NaBrO_3$ platelet is shown in Fig. 10. The crystals have the same crystallographic orientation, the opposite absolute atomic configuration, the opposite sense of piezoelectric voltage, and the same sense of optical activity. The interference curve is consistent only with the same sign for the nonlinear susceptibility.

The calculations of Endeman[19] have demonstrated that the optical activity is a very sensitive function of the lattice parameters describing the location of the oxygen triangles. In particular, a small variation in the azimuthal angle, i.e., a small rotation of the oxygen triangles around the [111] directions, may change the sign of the optical activity. This is the result of a detailed calculation which involves the dipole fields produced by the induced dipoles at each lattice site on other lattice sites. A general formulation of the local-field problem in second-harmonic generation has been given previously.[20] One may expect the nonlinear susceptibility also to be a sensitive function of the ionic positions. Since the odd-rank nonlinear polarizabilities of free centrosymmetric ions vanish, the calculation must start from orbitals which lack a well-defined parity due to the position of neighboring atoms. Since the nonlinear polarizabilities of such complexes are not known, a numerical solution of the local-field problem is not attempted here. An oversimplified starting point for such a calculation would be to consider the nonlinearity to reside exclusively in the O_3 triangles and represent these as a point in its center of gravity with a nonlinear polarizability. Such schematic models, however, can only be expected to give the order of magnitude, which is already known from Miller's rule.[9] The correct numerical value and the correct sign require a more detailed analysis of electronic structure and local-field configurations. Considerable variations induced by small changes in the structure parameters may be expected.

We have also related the sign of the nonlinear susceptibility of α-quartz to the sign in $NaClO_3$ by the interference experiment shown in Fig. 11. The absolute configuration of α-quartz and its relation to the sign of the piezoelectric effect[17,18] were used to determine the orientation of the quartz sample. All data concerning the sign of the third-rank tensors and the optical activity are summarized in Table II.

4. CONSERVATION OF ANGULAR MOMENTUM IN THE GENERATION OF CIRCULARLY POLARIZED HARMONIC LIGHT QUANTA

Since in each elementary scattering process two right (left) circularly polarized fundamental quanta are anni-

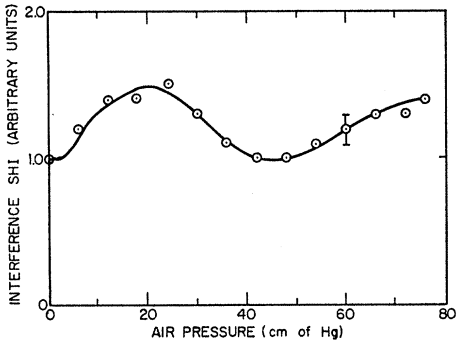

FIG. 10. Second-harmonic interference intensity from one dextrorotatory $NaClO_3$ (111) crystal and one dextrorotatory $NaBrO_3$ (111) crystal versus air pressure.

[17] W. G. Cady *et al.*, Proc. IRE **37**, 1384 (1949).
[18] A. De Vries, Nature **181**, 1193 (1958).
[19] H. J. Endeman, Academisch Proefschrift, Utrecht, 1965 (unpublished). See also Ref. 14.
[20] J. A. Armstrong, N. Bloembergen, J. Ducuing, and P. S. Pershan, Phys. Rev. **127**, 1918 (1962) (see especially the Appendix).

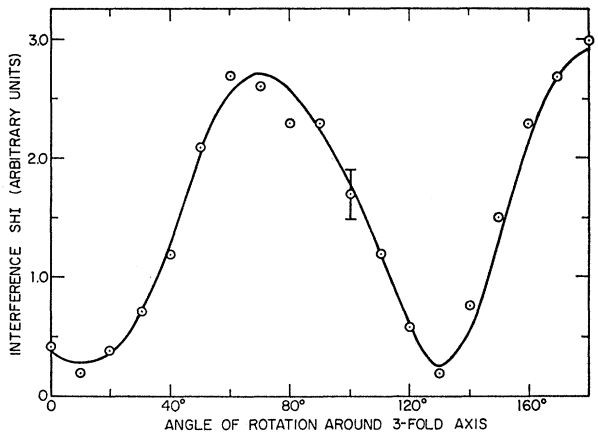

Fig. 11. Second-harmonic interference intensity from a dextrorotatory $NaClO_3$ (111) crystal and a levorotatory α-quartz (c-axis) crystal versus relative rotation around the threefold axis.

hilated and one left (right) circularly polarized quantum is created, the angular momentum of the electromagnetic field[21] is changed in the experiments described in this paper. It has been briefly shown elsewhere[6] that total angular momentum is conserved in this process because the light fields exert a torque on the crystalline lattice. In this section, we shall expand the previous discussion, which was based on the explicit introduction of the crystalline-field potential on electronic orbitals of localized ions, and we shall also give an alternate description in terms of Bloch wave functions.

A. Ionic Model with Trigonal Crystal Field

Consider an ion subjected to a crystal field of threefold symmetry around the $\hat{z}$ axis and lacking inversion symmetry. The crystal-field potential may be expanded as follows:

$$V_{cr}=\sum_{l=2}^{\infty} B_{l,0}Y_l^0+\sum_{l=3}^{\infty} B_{l,\pm 3}Y_l^{\pm 3}+\cdots, \qquad (5)$$

where Y_l^m is the normalized spherical harmonic function with the threefold axis as polar axis, and $B_{l,\pm 3}=B_{l,\mp 3}{}^*$. There may also be terms in $Y_l^{\pm 6}$, etc., whose presence would not alter the following argument.

The azimuthal variation of Y_l^m around this axis is given by $\exp[\pm 3i(\phi_e+\phi_L)]$. Here ϕ_e is the azimuth angle of the electron position with respect to the crystallographic x axis, and ϕ_L determines the position of the x axis with respect to a fixed laboratory frame, in which the crystal is allowed to rotate. In most problems the coordinate of the whole lattice ϕ_L is suppressed, but it is important in the discussion of the conservation of angular momentum.

Let ψ_g be the ground-state orbital wave function of a valence electron in the ion. In a nonmagnetic material this wave function may be chosen as real, because V_{cr} is real, and it should also exhibit the threefold symmetry:

$$|g\rangle=\psi_g=\sum_{l=0}^{\infty} c_{l,0}Y_l^0+\sum_{l=3}^{\infty} c_{l,\pm 3}Y_l^{\pm 3}+\cdots. \qquad (6)$$

The electric dipole interaction describing the interaction with a circularly polarized light wave propagating in the same z direction may be written in the form

$$-e\mathbf{r}\cdot\mathbf{E}_{r.c.}=Ca_r{}^{\dagger}Y_1^{-1}+C^*a_rY_1^{+1}, \qquad (7)$$

where $a_r{}^{\dagger}$ and a_r are the annihilation and creation operators for a right circularly polarized quantum and C is a c number, containing the appropriate numerical constants. For a left circularly polarized quantum the operator $a_r{}^{\dagger}$ is replaced by a_l and a_r by $a_l{}^{\dagger}$. From here on, we shall assume that the fundamental field is right circularly polarized and the harmonic field left circularly polarized. The harmonic production is described by third-order perturbation theory involving matrix elements of the form

$$\langle g|C^*Y_1^{+1}|n\rangle\langle n|C^*Y_1^{+1}|n'\rangle \times\langle n'|C^*Y_1^{+1}|g'\rangle a_r(\omega)a_r(\omega)a_l{}^{\dagger}(2\omega). \qquad (8)$$

The final state $|g'\rangle$ must be identical to the nondegenerate electronic ground state $|g\rangle$. Here $|n\rangle$ and $|n'\rangle$ are virtual intermediate excited states. It is readily seen that a spherical harmonic Y_l^m in the ground-state wavefunction expansion is carried over into a term $Y_{l'}{}^{m'}$ with $m'=m+3$ and $l'=l\pm 1$ or $l'=l\pm 3$. The third-order matrix elements will not vanish if, and only if, the expansion for $|g\rangle$ contains both even and odd l, and contains terms differing by three units of the azimuthal quantum number. The first condition is met, because the crystalline-field potential lacks inversion symmetry and contains terms with B_l with odd l. The second condition is met because the axis has threefold symmetry.

TABLE II. Sign of odd-rank tensor elements in piezoelectric optically active crystals.

Crystal	Absolute configuration	Optical activity	Nonlinear susceptibility	Piezoelectric constant
α-quartz	right-handed spiral[a]	levo	+[b]	−[c]
$NaClO_3$	A[d]	dextro	+	+
$NaBrO_3$	inverted A	dextro	+	−

[a] See Ref. 18.
[b] The sign in levorotatory quartz is arbitrarily taken as positive. Only the relative signs in this column are accessible to experimental determination at present. The absolute sign of the dc electro-optic effect may be determined by applying a dc electric field of known direction to an absolute configuration of known orientation. The optical nonlinearity may then be followed as a function of frequency through the infrared dispersion region, as has been done for example in GaP [W. L. Faust and C. H. Henry, Phys. Rev. Letters 17, 1265 (1966)]. When the absolute sign of the nonlinearity of one crystal has thus been determined in the optical region, the sign in other crystals may be compared with it as described here. The outcome of such an experiment would decide whether all signs of the nonlinear susceptibility in this table should be reversed.
[c] See Ref. 17. In this reference "right" and "left" refer to the atomic arrangement or the appearance of natural crystal faces and not to optical activity. We have used Mason's results, as quoted in *American Institute of Physics Handbook* [(McGraw-Hill Book Co., Inc., New York, 1963), 2nd ed., pp. 9–97 and 98], to unambiguously orient our $NaClO_3$ and $NaBrO_3$ crystals, and we have assumed that his measurements were made in accordance with the definitions in Ref. 17.
[d] Defined by Fig. 8.

[21] A. Messiah, *Quantum Mechanics* (North-Holland Publishing Co., Amsterdam, 1962), Vol. II, Chap. 23.

Note that the light wave interacts only with the electrons and the spherical harmonics in Eq. (7) have the azimuthal dependence $\exp(\pm i\phi_e)$. The crystal-field dependence in Eq. (5) which is responsible for the wave functions (6) has the angular dependence $\exp\pm i(\phi_e+\phi_L)$, if the lattice position coordinate is explicitly retained. The final state $|g'\rangle$ differs from the initial state $|g\rangle$ by a factor $\exp(3i\phi_L)$. This implies that the crystal lattice as a whole has changed its angular momentum by an amount

$$\left\langle \psi_L^* e^{-3i\phi_L} \left| -i\hbar \frac{\partial}{\partial \phi_L} \right| \psi_L e^{+3i\phi_L} \right\rangle - \left\langle \psi_L^* \left| -i\hbar \frac{\partial}{\partial \phi_L} \right| \psi_L \right\rangle = 3\hbar. \quad (9)$$

Through the intermediary of the crystalline potential the circularly polarized harmonic generation exerts a torque on the lattice, so that total angular momentum is conserved.

B. Rotational Doppler Shift

The rotational kinetic energy of the lattice associated with this angular momentum is, of course, negligible due to the large moment of inertia $\mathcal{I}$ of the lattice. If the lattice is initially at rest, the rotational velocity after one second-harmonic quantum has been created would be $\Delta\omega=3\hbar/\mathcal{I}$ and the associated kinetic energy would be $\frac{1}{2}\mathcal{I}\Delta\omega^2=9\hbar^2/2\mathcal{I}$. In principle, the emitted second-harmonic quantum would be shifted down in energy, but this is unobservable. In practice, the suspension of the crystal would compensate for the torque exerted by the light fields. For crystal plus suspension $\mathcal{I}\rightarrow\infty$.

If, however, the crystal is freely rotating and has initially an appreciable angular velocity ω_L, the change in kinetic energy would be

$$\hbar\Delta\omega_D=\mathcal{I}\omega_L\Delta\omega_L=3\hbar\omega_L. \quad (10)$$

The circularly polarized harmonic light would experience a rotational Doppler shift $\Delta\omega_D$ equal to three times the rotational velocity of the crystal. This Doppler shift is toward higher frequencies when the lattice is spinning in a direction opposite to the sense of precession of the fundamental circulation. This effect could also be derived from a simple kinematic consideration in a reference frame where the crystal is at rest.

C. Higher Harmonics; Axes of Fourfold and Sixfold Symmetry

These considerations may readily be extended to axes of fourfold or sixfold symmetry and to situations involving higher-harmonic or other combination frequencies. For a circularly polarized fundamental light beam propagating along a fourfold axis, no second harmonic can be created. The third-order perturbation by the EM fields could only connect states which differ in azimuthal quantum number by $\Delta m=\pm1$ (if the harmonic has the same sense of circulation as the fundamental) or $\Delta m=\pm3$, while the crystalline-field potential only mixes states with $\Delta m=0$ or $\Delta m=\pm4$.

The third harmonic may, however, be created in this case with a circulation in the opposite sense from the fundamental polarization. If two beams at ω_1 and ω_2 are incident with the same sense of circular polarization, it is possible to generate the combination frequencies $2\omega_1+\omega_2$ and $2\omega_2+\omega_1$, with the opposite circulation, because these optical processes correspond to $\Delta m=\pm4$ transitions. Quanta at $2\omega_1-\omega_2$ and $2\omega_2-\omega_1$ may be created with the same sense of circulation, since this corresponds to $\Delta m=0$ transitions.

If the beams at ω_1 and ω_2 have opposite circulation, then $2\omega_1+\omega_2$ may be created with the same sense of polarization as ω_1 and $2\omega_2+\omega_1$ with the same sense as ω_2. This corresponds to $\Delta m=0$ transitions. Circularly polarized quanta at $2\omega_1-\omega_2$ should have the same sense as ω_2 in this case, corresponding to a $\Delta m=\pm4$ transition. Similarly, quanta at $2\omega_2-\omega_1$ would have the same circulation as ω_1. It is also clear that processes involving four circularly polarized quanta cannot occur for propagation along a threefold axis. The intensity for the third-harmonic production in quartz, discussed in Ref. 5, vanishes.

The considerations for second-harmonic generation along a sixfold axis, as may occur in the piezoelectric classes $\bar{6}$ and $\bar{6}m2$, are similar to those for the trigonal classes 3 and $3m$, respectively. The unit cell with a sixfold axis of rotation-inversion will contain two ions on sites with trigonal symmetry which are related to each other by the inversion operation. The second-harmonic polarization created by each ion would be 180° out of phase because the two sites have equal nonlinear polarizabilities with opposite sign. There is, however, another 180° phase shift, because the trigonal field at one site is shifted by an azimuthal angle of 60° with respect to the other. This effect is identical to that represented by the experimental data in Fig. 7. Thus, the second-harmonic polarizations of the two sites in the hexagonal unit cell add up in phase.

In the case of $\bar{6}$ or 3 symmetry, there is no plane of symmetry through which the rotating fundamental field vector and the counter-rotating second-harmonic polarization must pass at the same time. The second-harmonic polarization produced by a fundamental field circularly polarized around the axis of symmetry is described as follows[1,2]:

$$\mathbf{E}=(\hat{x}+i\hat{y})Ae^{-i\phi}e^{-i\omega t}+\text{c.c.},$$
$$\mathbf{P}(2\omega)=2(\chi_{xxx}-i\chi_{yyy})(\hat{x}-i\hat{y})A^2e^{-2i\phi}e^{-2i\omega t}+\text{c.c.}$$

The ratio of the two independent elements of the non-

linear tensor (χ_{xxx}/χ_{yyy}) determines the orientation of the plane of crossing of the two counter-rotating vectors.

In isotropic fluids any direction of propagation is an axis of infinitesimal symmetry. Only $\Delta m=0$ transitions are allowed. Circularly polarized light cannot produce third harmonics, while it may do so in cubic crystals propagating along the cubic axis.

If the light propagates along an arbitrary direction $\mathbf{K}$ in the crystal, the crystalline-field potential[5] may be expanded in spherical harmonics with this direction $\mathbf{K}$ as polar axis. The transformation formulas for the harmonics will in general allow all possible m values to occur, $Y_l^{m(\mathbf{K})}$. There are, therefore, no clearcut Δm selection rules in this case. The resulting harmonic and combination frequencies propagating along $\mathbf{K}$ will in general have elliptical polarization. It should be clear from the foregoing argument that the crystalline lattice, through the intermediary of the crystalline potential, will pick up whatever angular momentum is lost by the electromagnetic fields.

D. Polarization Selection Rules in a Band Model

The question of Δm selection rules may also be discussed in terms of band theory. The nonlocalized wave functions of the completely filled valence band are of the Bloch type $u_{n\mathbf{k}}(\mathbf{r})\exp(i\mathbf{k}\cdot\mathbf{r})$. The index n denotes the valence band. The light propagates with a wave vector $\mathbf{K}=|K|\hat{z}$ in the direction of a threefold axis of symmetry. Denoting the rotation operation around this axis by R_3 (where $R_3^3=\mathbf{I}$), one may consider the three degenerate electron states which form a star in $\mathbf{k}$ space[22]

$$\begin{aligned}\psi_{n,\mathbf{k}}(\mathbf{r})&=u_{n,\mathbf{k}}(\mathbf{r})e^{ik_z z}e^{i(\mathbf{k}_\perp\cdot\mathbf{r})},\\ \psi_{n,\mathbf{k}}(R_3^{-1}\mathbf{r})&=u_{n,R_3\mathbf{k}}'(\mathbf{r})e^{ik_z z}e^{i(R_3\mathbf{k}_\perp)\cdot\mathbf{r}},\\ \psi_{n,\mathbf{k}}(R_3\mathbf{r})&=u_{n,R_3^{-1}\mathbf{k}}''(\mathbf{r})e^{ik_z z}e^{i(R_3^{-1}\mathbf{k}_\perp)\cdot\mathbf{r}}.\end{aligned}\tag{11}$$

The primes are simply a reminder that the u's obtained by the symmetry transformation may differ by a phase factor.

The following linear orthonormal combinations are the appropriate zero-order wave functions in a crystal with optical activity. They are also the appropriate starting point for a perturbation by circularly polarized light waves,

$$\begin{aligned}\psi_{n,\mathbf{k}}{}^0&=3^{-1/2}[\psi_{n,\mathbf{k}}(\mathbf{r})+\psi_{n,\mathbf{k}}(R_3\mathbf{r})+\psi_{n,\mathbf{k}}(R_3^{-1}\mathbf{r})],\\ \psi_{n,\mathbf{k}}{}^1&=3^{-1/2}[\psi_{n,\mathbf{k}}(\mathbf{r})+e^{2\pi i/3}\psi_{n,\mathbf{k}}(R_3\mathbf{r})\\ &\qquad+e^{-2\pi i/3}\psi_{n,\mathbf{k}}(R_3^{-1}\mathbf{r})],\\ \psi_{n,\mathbf{k}}{}^{-1}&=3^{-1/2}[\psi_{n,\mathbf{k}}(\mathbf{r})+e^{-2\pi i/3}\psi_{n,\mathbf{k}}(R_3\mathbf{r})\\ &\qquad+e^{+2\pi i/3}\psi_{n,\mathbf{k}}(R_3^{-1}\mathbf{r})].\end{aligned}\tag{12}$$

The perturbation by a circularly polarized light wave will connect the state $\psi_{n\mathbf{k}}(\mathbf{r})$ to a conduction-band state $\psi_{n',\mathbf{k}+\mathbf{K}}(\mathbf{r})$. The $\mathbf{k}$ star in the valence band will be connected to the $\mathbf{k}$ star in the conduction band:

$$\begin{aligned}\psi_{n',\mathbf{k}+\mathbf{K}}(\mathbf{r})&=u_{n',\mathbf{k}+\mathbf{K}}(\mathbf{r})e^{i(k_z+|K|)z}e^{i\mathbf{k}_\perp\cdot\mathbf{r}},\\ \psi_{n',\mathbf{k}+\mathbf{K}}(R_3^{-1}\mathbf{r})&=u_{n',\mathbf{k}+\mathbf{K}}(R_3^{-1}\mathbf{r})e^{i(k_z+|K|)z}e^{iR_3\mathbf{k}_\perp\cdot\mathbf{r}},\\ \psi_{n',k+K}(R_3\mathbf{r})&=u_{n',\mathbf{k}+\mathbf{K}}(R_3\mathbf{r})e^{i(kz+|K|)z}e^{iR_3^{-1}\mathbf{k}_\perp\cdot\mathbf{r}}.\end{aligned}\tag{13}$$

Since the interaction Hamiltonian with a circularly polarized light wave is invariant for the symmetry operation R_3, the matrix element connecting the respective members of the two stars must be equal, except for a phase factor. In the electric dipole approximation the interaction may be written again in the form of Eq. (7). The operation R_3 carries ϕ occurring in the spherical harmonic $Y_l^{\pm1}$ into $\phi+\frac{2}{3}\pi$. This symmetry operation transforms the matrix element according to

$$\begin{aligned}R_3^{-1}\int u_{n',\mathbf{k},\mathbf{K}}{}^*(R_3\mathbf{r})Ca^\dagger e^{i\omega t-i\phi}u_{n,\mathbf{k}}(R_3\mathbf{r})d^3r\\ =e^{+2\pi i/3}\int u_{n',\mathbf{k}+\mathbf{K}}{}^*(\mathbf{r})Ca^\dagger e^{i\omega t-i\phi}u_{n,k}(\mathbf{r})d^3r.\end{aligned}\tag{14}$$

The phase factors between corresponding matrix elements of the two $\mathbf{k}$ stars in the n and n' bands are given by $\exp(\pm\frac{2}{3}\pi i)$. If new linear combinations $\psi_{n',\mathbf{k}+\mathbf{K}}{}^0$, $\psi_{n',\mathbf{k}+\mathbf{K}}{}^{+1}$, and $\psi_{n',\mathbf{k}+\mathbf{K}}{}^{-1}$ are formed from Eq. (13) in the same way, as was done for the valence band in Eqs. (11) and (12), it is seen that the interaction with a circularly polarized wave connects $\psi_{n,\mathbf{k}}{}^0$ with $\psi_{n',\mathbf{k}+\mathbf{K}}{}^{+1}$, $\psi_{n,\mathbf{k}}{}^1$ with $\psi_{n',\mathbf{k}+\mathbf{K}}{}^{-1}$, and $\psi_{n,\mathbf{k}}{}^{-1}$ with $\psi_{n',\mathbf{k}+\mathbf{K}}{}^0$. We may say that $\Delta m=+1$ transitions occur between the two $\mathbf{k}$ stars, if a right circularly polarized quantum is annihilated or a left circular quantum is created. Conversely we have $\Delta m=-1$ transitions for the opposite senses of polarization. Similar $\mathbf{k}$ stars may be defined in a second conduction band n''. The annihilation of two right circularly polarized laser quanta and the creation of one left circularly polarized harmonic quantum will lead by standard third-order perturbation theory back to the original electronic state in the valence band. Thus the same Δm selection rules also follow from a band model with nonlocalized electron wave functions. These band considerations can obviously be extended to third-harmonic generation circularly polarized around a fourfold axes and other cases.

The conservation of angular momentum is not clear in this description, because no azimuthal coordinate for the lattice was introduced. The situation is similar to the description of "umklapp processes" in the reduced zone scheme. The lattice takes up the balance in translational momentum, in units of $\hbar$ times a reciprocal lattice vector. In a similar manner the lattice here takes up angular momentum in units of $3\hbar$. The three-pronged stars in $\mathbf{k}$ space correspond to "reduced rotational zones."

[22] M. Tinkham, *Group Theory and Quantum Mechanics* (McGraw-Hill Book Co., New York, 1964), p. 279 ff.

5. CONCLUSION

The magnitude of the optical nonlinearity, responsible for second-harmonic generation, has been determined in the optically active crystals $NaClO_3$ and $NaBrO_3$. Although the crystals have nearly identical structure, the optical nonlinearity does not obey Miller's rule, indicating its sensitive dependence on local-field configurations. The sign of the nonlinearity has been related to the absolute atomic configuration. It is naturally opposite for optical antipodes of the same crystal. The sign in $NaBrO_3$ is opposite to that in $NaClO_3$ for the same configuration, again indicating sensitivity to local-field effects. Second-harmonic interference effects with circularly polarized beams also verify the existence of various symmetry properties and their relation to the question of conservation of angular momentum.

ACKNOWLEDGMENTS

We wish to thank Dr. H. Rabin and J. Wynne for several stimulating discussions. We are indebted to S. Maurici, who grew, cut, and polished most of the samples. We also thank Dr. D. I. Bolef who originally supplied the levorotatory $NaClO_3$ crystal.

Errata

Phonon-Assisted Tunneling in Bismuth Tunnel Junctions, L. ESAKI, L. L. CHANG, P. J. STILES, D. F. O'KANE, AND NATHAN WISER [Phys. Rev. **167**, 637 (1968)]. The following corrections and note added in proof did not appear in the published article: Bi-Al-$_2O_3$-Au and $5<10^{-4}$ cm^2 should be corrected to read Bi-Al_2O_3-Au and 5×10^{-4} cm^2, respectively. All MeV in the manuscript should read meV (millielectron volt). Page 639, left column, 3rd line from top, sentence "This is probably due to the larger number of single-crystal units." should be deleted.

Note added in proof. J. J. Hauser and L. R. Testardi recently published tunneling on bismuth [Phys. Rev. Letters **20**, 12 (1968)], where they failed to see fine structure in the low-energy range, as reported in Ref. 1 and also here. They emphasized that tunnel junctions should be judged from a superconducting criterion and apparently attributed the disagreement between their results and ours to their proper tunneling behavior.

If Pb is used instead of Au as a counterelectrode in our junctions, we always observe the superconducting energy gap of Pb and its disappearance with applied magnetic fields. The main structure described here, however, does not change with increase in magnetic fields up to 90 kOe. Thus, our junctions are comparable according to their criterion.

Therefore, we believe that the difference comes mainly from the quality of bismuth. We used bulk single-crystal bismuth while they always deposited a bismuth film on an oxidized metal stripe for tunneling experiments, which does not result in decent single-crystal bismuth. (As they reported, one can obtain reasonably good single crystals by depositing bismuth directly on NaCl or mica, which does not appear to be relevant to their tunneling results.) We think that a certain ratio of phonon-assisted tunneling to direct tunneling is required to see the band-edge effect in the low-energy range and this cannot be attained with such bismuth films. Our polycrystalline junction E-42 (Fig. 1) is indeed in good agreement with their results.

Investigation of Energy-Band Structures and Electronic Properties of PbS and PbSe, SOHRAB RABII [Phys. Rev. **167**, 801 (1968)]. In Table XII on page 807 the label "Theory" of column 2 should be deleted, and the labels "Experiment" and "Theory" of columns 3, 4 and 5, 6 should be interchanged. In Table XIII on p. 807 the label $|g_1|$ applies to both columns 4 and 5, and the label $|g_{100}|$ applies to columns 6, 7, and 8.